UFTP preprint 245/1990

Institut für Theoretische Physik
Johann Wolfgang Goethe Universität
Frankfurt am Main

String Dynamics in Hadronic Matter

H. Sorge, A. v. Keitz, R. Mattiello, H. Stöcker and W. Greiner

Institut für Theoretische Physik,
Johann Wolfgang Goethe-Universität,
D-6000 Frankfurt am Main 11, Postfach 11 19 32.

Work supported in part by Bundesministerium für Forschung und Technologie (BMFT), by Deutsche Forschungsgemeinschaft (DFG) and by Gesellschaft für Schwerionenforschung (GSI).

Institut für Theoretische Physik der Universität Frankfurt
Robert-Mayer-Str. 8-10, D-6000 Frankfurt am Main

String Dynamics In Hadronic Matter

H. Sorge, A. v. Keitz, R. Mattiello,
H. Stöcker and W. Greiner
Institut für Theoretische Physik
Johann Wolfgang Goethe Universität Frankfurt, Germany

Abstract

Hadron production in soft hadronic collisions is successfully described by a longitudinal excitation and subsequent decay of color flux tubes. We consider the dynamics of interacting unstable strings as a generalization designed for hA and AA interactions at ultrarelativistic energies. The constituent quarks at the ends of the decaying strings and the produced hadrons can interact with the surrounding matter. The effect of secondary interactions in molecular dynamics calculations for AA collisions at CERN energies ($200 A GeV$) can be seen in an enhancement of transverse energy, particle production and the mean transverse momenta. The results agree very well with the experimental measurements at ultrarelativistic beam energies in pp, hA and the recent AA collisions.

In the recent experiments at the CERN-SPS beams of light projectiles ($^{16}_{8}O$ and $^{32}_{16}S$) are accelerated up to 200 GeV per projectile nucleon. The main goal is to explore the properties of hot, dense hadronic and quark matter. However, little is known about the complicated dynamics in a collision of such a projectile with a heavy target – in particular about the first stages of the collision. A straightforward extension of the hadron physics to such a system does not exist. In fact, it is hoped that many-body effects like a possible phase transition into a quark gluon plasma do occur in heavy ion collisions, which are not expected for hadron-hadron interactions or in hadron-nucleus collisions [1].

To explore the dynamics of ultrarelativistic heavy ion collisions we have developped a microscopic phase space approach whose main features are described elsewhere [2]. The approach is dubbed "Relativistic Quantum Molecular Dynamics"(RQMD). The main ingredients are the Lorentz covariant classical propagation of all hadrons – the original nucleons and the secondaries – (molecular dynamics) combined with stochastic particle production and absorption in binary collisions or decays of hadrons.

In the RQMD approach two hadrons scatter if they pass during their propagation the minimum distance d in their two-body CMS with $d \leq \sqrt{\sigma/\pi}$. For the most frequent hadrons – nucleons, pions and kaons – the experimentally given total and elastic cross sections are used according to [3]. It is assumed that hadron production occurs by resonance formation, and the probabilities for the resonances in the outgoing channels are fixed by a fit to exclusive pion and kaon production data [4]. Very heavy resonances above a certain mass threshold are assumed to be excited into strings. The threshold e. g. for nonstrange baryons amounts to $2GeV/c^2$. The direction of the one-dimensional excitation is given in the two-particle CMS by the direction of hadron motion. The stringlike excitation and subsequent fragmentation has been shown to be a very reasonable model of high energy hadron production [5], both in hadronic and also for e^+-e^- and lepton-hadron interactions. For the string fragmentation we use the JETSET routines developped by the LUND group [6]. Some of the routines and default parameters have been modified, for instance to get a better description of strange baryon production [7]. The string excitation law for the outgoing hadrons is chosen by assuming a scaling law for the probability distribution of the new light cone momenta. The light cone momenta are defined as $p^{\pm} = p^0 \pm p_l$. The longitudinal direction refers to the direction of ingoing hadron motion in the two-hadron CMS. In the collision both particles get new momenta

$$\begin{aligned} (p_1^+, p_1^-) &\longmapsto (p'^+_1, p'^-_1) \\ (p_2^+, p_2^-) &\longmapsto (p'^+_2, p'^-_2). \end{aligned} \tag{1}$$

The old light cone momentum pair has a large and a small component for every particle (depending on the sign of p_l). The new value of the small light cone component scales according to the probability distribution

$$dP \sim \frac{dp'^{\pm}}{p'^{\pm}} \quad .$$

The other component is given by momentum conservation. One can easily see that for the case of diffractive scattering this results in a probability distribution of the form

$$dP(M^2) \sim \frac{d(M^2)}{M^2}.$$

This scaling law has experimentally been observed in a missing mass analysis of diffractive collisions at very high energies [8].

Note that during the dynamical evolution a large number of unstable hadrons are produced. For cross sections in experimentally not accessible reactions – e.g. $\Delta^+\Omega^{*-}$ – we assume

$$\sigma_{tot} \;=\; 40 \cdot (2/3)^{n_m} \cdot (1 - 0.4x_1(S)) \cdot (1 - 0.4x_2(S))\text{mb}$$

$$\sigma_{el} = c(s) \cdot \sigma_{tot}^{3/2}$$
$$\frac{d\sigma_{el}}{dt} \sim \exp(bt) \qquad b \sim \sigma_{tot}^{1/2}$$

with n_m the number of ingoing mesons, $x_i(S)$ the fraction of ingoing strange quarks and t and s the Mandelstam variables. $c(s)$ is independent from the interacting hadron species. These relations give good agreement with the high energy behavior in the known hadronic collisions [8]. The formula for σ_{el} represents only the high energy limit, because for the mass excitation according to eq.(1) a minimum excited mass is required, otherwise the mass remains nonexcited. Baryon annihilation has also been incorporated into the RQMD model – with the experimentally determined cross sections and an extrapolation to unstable and strange baryons.

How long does it last until a secondary hadron materializes and interacts with its environment? Unfortunately, we cannot get this information from first principles, because the hadronization is a soft process – determined by the nonperturbative regime in QCD. Even worse, for a composite object like a hadron the different parts of the hadron may begin to interact at different times. We have to start with phenomenological models – see for instance [14]-[18] – and test them against the experimental data. First the experimentally available information from hadron-nucleus interactions is used as a probe of the space-time structure of hadronic interactions.

The decay law of an excited string is formulated in momentum space. It fixes the production points of the $q\bar{q}$ pairs where the color flux tube breaks (in the yo-yo picture). There is no unique extrapolation for the case of subsequent interactions, if the string does not decay in the vacuum but in hadronic matter. The question is: which parts of the excited object after the first collision can interact with which interaction probability and which (de-)excitation scheme? In some models only the outgoing leading hadrons can interact furtheron, either with a modified excitation scheme [9] or the same as used for the first collision [10]. In other approaches the excited projectile is kept stable using the same interaction probabilities and excitation scheme afterwards. Its decay – after its propagation through the target – is independent from the other excited target nucleons [11, 12]. In more sophisticated approaches the string can be deexcited by stochastic decay before colliding once more. This allows to take rescattering of produced secondaries into account, either covariantly as in the original RQMD model [2] or nonrelativistically by choosing an appropriate observer frame [13].

In the original RQMD calculations the string itself gets a finite life time – with the width $\Gamma = 0.1 \cdot$ mass. Its total energy-momentum can be used to excite target nucleons by loosing momentum. Now, in the modified RQMD approach only the – "dressed" – constituent quarks sitting at the ends of the color flux tube can interact furtheron with the target. Their reaction cross sections are taken in accord with the additivity hypothesis of the additive quark model (AQM): 1/3 (q in a baryon), $\approx$1/2 (q in a meson) or 2/3 (diquark

in a baryon) of the corresponding hadron nucleon cross section [17].

This AQM description is favored by the experimentally observed A-dependence for fast (anti-) proton production in πA collisions [19]. The main idea is to relate the nuclear attenuation of different leading baryons to the interaction probability of the excited projectile and the formation time of the asymptotic state. The use of a pion beam is preferable as compared to a proton beam, because in the latter case the diffractive interactions of the projectile distort the clean picture of baryon formation by creating quarks from the sea. The outgoing (anti-) protons have been measured at a Feynman-x around 0.5 with a pion beam of 30 GeV/c. If one looks at baryons with high x-values target contributions should be neglegible, and there is a large probability that one of the original valence quarks combines with a produced diquark. The longer the intermediate state behaves like a pion the weaker should be the difference between the attenuation of the proton and the antiproton. In the extreme case that the asymptotic hadrons are formed outside the target there should be no flavor dependence in the attenuation. In contrast, the additive quark model predicts the strongest flavor dependence of attenuation which is in accordance with the data. The reason is that the $\overline{q}$ nucleus reaction is more probable than the q reaction which is related to the larger $\overline{N}N$ – compared to NN – cross section because of possible annihilation.

The deceleration of the produced hadrons should not only depend on the dressed quark-nucleon interaction but also on the position at which the produced hadrons begin to interact in the target. In the present model it is assumed that the formation time is associated with the finite time, needed to break the color flux tube by pair production. The space-time point from which a produced hadron begins to propagate is the arithmetic mean of the two space-time points at which the string breaks. This time amounts to an average time of 0.9-1.2 fm/c in the rest system of the hadron depending on the reaction under consideration. The string tension which enters inversely into the formula for the formation point gets its "canonical value" of $1 GeV/\mathrm{fm}$. We use a slightly different prescription of the formation point for those hadrons which contain the constituent quarks of the decaying string. If we analogously average the turning point of the yo-yo endpoint and the first breakpoint of the string a minimum time would exist before such a hadron could not be formed. This is due to the turning point of the quark which leads to a minimum formation time of $\frac{m_t}{\sqrt{2}\kappa}$. Instead, in RQMD their formation time is stochastically given by an exponential distribution with the same mean value as above. This may account for the transverse growth of the string which to a large extent determines the cross section of the formed hadron.

We had to use some simplifications in the RQMD Monte Carlo code to sample enough statistics in the pion-nucleus case. The pion string was forced to produce a diquark at its first break point (from the left or right side). A second simplification was to take only the participant nucleons into account. In general the nucleons are bound together by quasi-potential forces [2] which were substituted in this case by freezing the nucleons' Fermi

momenta. Fig.1 shows the RQMD results in comparison with the data [19] for the ratio R

$$R = \frac{d\sigma(\pi^- A \to p \text{ or } \overline{p})/dx|_{x=0.5}}{d\sigma(\pi^- p \to p \text{ or } \overline{p})/dx|_{x=0.5}}$$

as a function of the target mass A. The formation point concept described above yields good agreement with the data. The defined mean formation time in the RQMD approach is – in the target frame – in between the "constituent formation time" and the "yo-yo time" discussed in [18]. There the authors found that the hadron formation based on the constituent time agrees well with the experimentally observed (anti-) baryon attenuation in πA collisions while the yo-yo time gives a slightly too small attenuation. Note that the RQMD calculations – with a larger mean formation time – can result in nearly the same attenuation, because the exponential distribution of formation points populates short times more frequently than the constituent time ansatz. The different stochastic distributions become important, because only the formation points inside the target are relevant for attenuation.

The constituent (di-) quarks at the ends of a decaying string can interact before the string has broken and the new daughter hadrons which contain these (di-) quarks have been formed. It is important how the interactions with the constituent quarks are implemented. In RQMD it is assumed that the excitation scheme in a binary collision is the same as used for hadronic interactions. Therefore one has to specify which portion of the total energy-momentum of the string is carried by these constituents and is available in subsequent collisions. Because of lacking knowledge we assume that this momentum distribution is the same as for the corresponding hadrons which are formed at the ends of the string. In fact, in ultrarelativistic hA collisions the dressed quark-hadron interactions are by far more important than the interactions of hadrons after their formation in the target matter. Fig.2 shows for a p A reaction that most of the produced particles are either produced in the first collision of the ingoing proton or in collisions of constituent (di-) quarks. This has been demonstrated in the model by blocking all collisions with hadrons *after* their formation. The number of produced negatively charged particles for instance decreases in this case (p + Xe) from 6.8 to 6.5 only.

We see from Fig.2 that the RQMD calculations give good agreement with experimentally measured rapidity distributions [20] for p Ar and p Xe reactions. The string fragmentation parameters have been fixed to pp data in a broad energy range. The experimentally observed fluctuations [20] in the multiplicity distributions are also well reproduced by the RQMD calculations (see Fig.3).

The RQMD approach had formerly also been applied to heavy ion collisions at AGS energies (10 to 15 $AGeV$) [2, 21]. There it was demonstrated that the rescattering of produced hadrons is an essential aspect of the dynamics in a collision at these energies. Can we see the importance of rescattering also at CERN energies? Or does the finite formation time multiplied with the Lorentz dilation ($\gamma = 10$ for particles at midrapidities) spoil the

rescattering? This was first studied in [2] where a strong effect on baryon distributions had been predicted.

In Fig.4 we compare the produced transverse energy for RQMD and FRITIOF calculations with the experimental data [22]. FRITIOF is an independent fragmentation model whose string fragmentation parameters are tuned to pp and pA collisions [11]. In contrast to the pp and the pA case FRITIOF slightly underestimates the particle production and transverse energy in AA collisions [22]. This is related to the neglect of rescattering. However, we can see in Fig.4 that the effect is small for the transverse energies in the forward angular cone ($\eta > 2.4$ means $\theta < 10.4^o$), because the very fast hadrons are contained here which are less affected by rescattering.

It is expected that near midrapidity the rescattering of secondaries – or other hadron and quark matter effects – is clearly visible in the experimental data. In Fig.5 the calculated mean collision numbers in central S($200AGeV$) + S collisions are shown for different hadron species. Here one observes a clear correlation between rapidity and collision frequency. The NA35 group measured recently the charged particle yields in the rapidity bin $2 < y < 3$ ($y = 3$ is midrapidity) in the reactions O on Au and S on S [23] at $200AGeV$. We show the NA35 rapidity distribution and the transverse momentum spectra of the negatives in Fig.6 together with the RQMD results.

In Fig.6 we compare the RQMD results with the default description for the formation time with a calculation in which all particles are produced without time delay. While the original RQMD calculation agrees with the NA35 data, setting the formation time to zero produces by far too many particles. This clearly demonstrates the importance of the formation time for suppressing particle production.

The NA35 group found that one cannot fit the transverse momentum spectra with one exponential, but has to use a "two temperature fit" for a source at rest in midrapidity with $T_1 = 43$ MeV and $T_2 = 153$ MeV and $N_1/N_2 = 0.23$ (in the case of the O + Au collisions). The "low temperature" pions might be caused by low mass resonance decay and effective masses for nucleons and mesons in dense matter. A detailed analysis of their sources in the framework of the RQMD approach is in progress [24]. The "high temperature" pions show a larger p_t-slope than in the pp data (135 MeV). (Note that there is no particle identification in the experiment which causes some misidentification of heavier particles – K^-, $\overline{p}$ – as pions.) The phenomenon of transverse momentum enhancement can also be seen in the RQMD calculations for the negatively charged particles. The calculated mean transverse momentum at midrapidity is about 35 MeV larger than the corresponding value in pp collisions (375 to 340 MeV). The analysis of the RQMD calculations shows that in the mean 35% of the produced mesons near midrapidity collided once or more. This shifts their transverse momenta to higher values. Rescattering can also be seen better at higher p_t values if strangeness production is studied: The ratios of strange to nonstrange mesons increases much faster with higher p_t values than in elementary collisions [21].

Fig.7 shows the calculated angular distributions of the protons and all charged particles for central O + Au collisions. Here we compare the calculation with default description for hadron formation with a RQMD calculation in which the formation time has been set to infinity. We observe that the default description results in more particle production and more protons with a kinetic energy above 40 *MeV*. The enhancement at low pseudo-rapidities signals the influence of cascading in the target.

In conclusion we have demonstrated that rescattering is important in reactions like O + Au or S + S at CERN energies. Secondary interactions enhance the produced transverse energy, the particle production and mean transverse momenta. This can be seen by comparing the RQMD calculations and the experimental data with calculations without secondary interactions. However, the finite formation time leads to a strong suppression of the rescattering effects. One has to look at specific windows in phase space and at central collisions to see the effects of hadron rescattering. Multiple collisions per hadrons ensure that a system starts to equilibrate which might be suited to search for the most interesting collective effects. For light projectiles the surface to volume ratio is rather large. This enlarges the difficulty to disentangle the – interesting – multi-hadron (or even multi-quark and -gluon) effects from the "ordinary" pp-like physics. Therefore it is of vital importance that the most massive nuclei are colliding (i. e. Pb + Pb) if collective effects – e. g. the formation of a quark gluon plasma – are to be searched for.

References

[1] For a review and further references see: H. Stöcker, W. Greiner: Phys.Rep. 137(1986)

[2] H. Sorge, H. Stöcker, W. Greiner: Ann. of Phys. 191(1989) 266; H. Sorge, H. Stöcker, W. Greiner: Nucl.Phys. A498 (1989) 567c

[3] Particle Data group: LBL-100 Revised UC-34d (1982)

[4] J. Bystricky et al: DPhPE 87-03,Saclay 1987 G. Bertsch, M. Gong, L. McLerran, V. Ruuskanen, E. Sarkkinen: Phys.Rev. D37(1988) 1202; A.M. Rossi et al.: Nucl.Phys. B84(1975) 269; C.B. Dover, G.E. Walker: Phys.Rep. 89(1982) 1

[5] B. Andersson, G. Gustafson, G. Ingelman, T. Sjöstrand: Phys.Rep. 141(1983) 31; X. Artru: Phys.Rep. 141(1983) 147

[6] T. Sjostrand: Comp.Phys.Comm. 39(1986) 347

[7] R. Mattiello, H. Sorge, H. Stöcker, W. Greiner: manuscript in preparation

[8] K. Goulianos: Phys. Rep. 101(1983) 169

[9] A. Klar, J. Hüfner: Phys. Rev. D31(1985) 491; L. P. Csernai, J. I. Kapusta: Phys. Rev. D31 (1985) 2795; R. C. Hwa: Phys. Rev. Lett. 52 (1984) 492

[10] C. Y. Wong: Phys. Rev. Lett. 52 (1984) 1393; J. Ranft: Phys. Rev. D37 (1988) 1842; A. Shor, R. Longacre: Phys. Lett. B218 (1989) 100

[11] B. Andersson, G. Gustafson, B. Nilsson-Almqvist: Nucl.Phys. B281(1987) 289; B. Nilsson-Almqvist, E. Stenlund: Comp. Phys. Comm. 43(1987) 387

[12] K. Werner: Phys. Rev. D39 (1989) 780

[13] K. Werner, P. Koch: CERN-TH-5607/89

[14] L. Landau, I. Ya. Pomeranchuk: Dokl. Akad. Nauk. 92(1953) 535; E. L. Feinberg , I. Ya. Pomeranchuk: Nuovo Cim. Suppl. 3 Ser.10 (1956) 652

[15] G. Bialkowski, C. B. Chiu, D. M. Tow: Phys. Rev. D17(1978) 862

[16] K. Gottfried: Phys. Rev. Lett. 32(1974) 957; F. E. Low, K. Gottfried: Phys. Rev. D17(1978) 2487

N. N. Nikolaev: Z. f. Phys. C5(1980) 291

[17] A. Bialas, M. Bleszynski, W. Czyz: Nucl. Phys. B111(1976) 461; A. Bialas, W. Czyz, L. Lesniak: Phys. Rev. D25(1982) 2328; A. Bialas, W. Czyz, L. Lesniak: Z. f. Phys. C13(1982) 147

[18] A. Bialas, M. Gyulassy: Nucl. Phys. B291(1987) 793

[19] M. G. Abreu et al.: Z. f. Phys. C25(1984) 115

[20] C. de Marzo et al.: Phys. Rev. D26(1982) 491, Phys. Rev. D29(1984) 363, Phys. Rev. D26(1984) 2476

[21] R. Mattiello, H. Sorge, H. Stöcker, W. Greiner: Phys. Rev. Lett. 63(1989) 1459

[22] H. R. Schmidt et al.(WA80): Z. f. Phys. C38(1988) 109

[23] H. Ströbele et al.(NA35): Z. f. Phys. C38(1988) 89; J. Harris et al.(NA35): Nucl. Phys. A498 (1989) 133c

[24] H. Sorge: manuscript in preparation

Figure captions:

Figure 1:

$$R = \frac{d\sigma(\pi^- A \to p \text{ or } \bar{p})/dx|_{x=0.5}}{d\sigma(\pi^- p \to p \text{ or } \bar{p})/dx|_{x=0.5}}$$

as a function of the target mass A. The momentum of the π^- projectile is $30GeV$. The data from [19] are symbolized by the circles ($\bar{p}$) and squares (p). The dashed line (for p) and the full line (for $\bar{p}$) are the RQMD calculation.

Figure 2: Charged particle rapidity distribution in p p, p Ar and p Xe collisions at E_{kin} =200GeV. The circles and the squares represent the data from [20], the full histograms the default RQMD calculation. All fast charged hadrons are counted as pions which leads to a misidentification for a subset of particles (protons, kaons). This misidentification has been simulated in the RQMD calculations. For the p Xe reaction the dashed curves show the results obtained by setting the hadron formation time to infinity.

Figure 3: Charged particle multiplicity distribution in p p, p Ar and p Xe collisions at E_{kin} =200GeV. The same conventions as in Fig.2 are used.

Figure 4: Differential cross section for transverse energy production in O(200 $AGeV$) on Au collisions in the pseudo-rapidity window $2.4 < \eta < 5.5$. The circles represent the data from [22], the dashed histogram the FRITIOF calculations and the full histogram the RQMD calculations for central and semi-central collisions ($b \leq 5$fm).

Figure 5: Mean collision number of nucleons (straight line), anti-nucleons (dashed line) and pions (dotted line) as a function of final rapidity. These distributions are calculated for central S(200 $AGeV$) on S collisions. Note that a large fraction of these collisions occur with constituent quarks before the final hadrons have been formed.

Figure 6: Comparison of rapidity distributions and transverse momentum spectra between experimental data [23] and RQMD calculations for central collisions of O(200 $AGeV$) on Au (left side) and S(200 $AGeV$) on S (right side). The experimental trigger includes only events with minimum energy flow in forward direction corresponding to a total cross section of 56 (35) mb. The figure a) (O + Au) shows the rapidity distributions of the negatively charged hadrons – dots are the data and histogram (bold lines) the RQMD

results – and of the nucleons (histogram with straight lines). The full line is the result of a calculation for the negatives with formation time set to zero. The figure b) (S + S) shows the rapidity distributions of the negatives – squares are the data and full line the RQMD results – and of the protons (histogram). The figure c) (O + Au) and d) (S + S) show the transverse momentum spectra for negatives in the rapidity interval $2 < y < 3$: triangles (RQMD) and crosses (data).

Figure 7: Comparison of charged particle angular distribution between experimental data [22] and RQMD calculations for central collisions of O(200 *AGeV*) on Au. The squares represent the WA80 data for all charged particles and the full circles for protons with a kinetic energy above 40 *MeV*. The straight lines (curve and histogram) are the corresponding results of the default RQMD calculations. Dashed curve (charged particles) and dotted histogram (protons) represent the results with infinite hadron formation time.

Figure 1

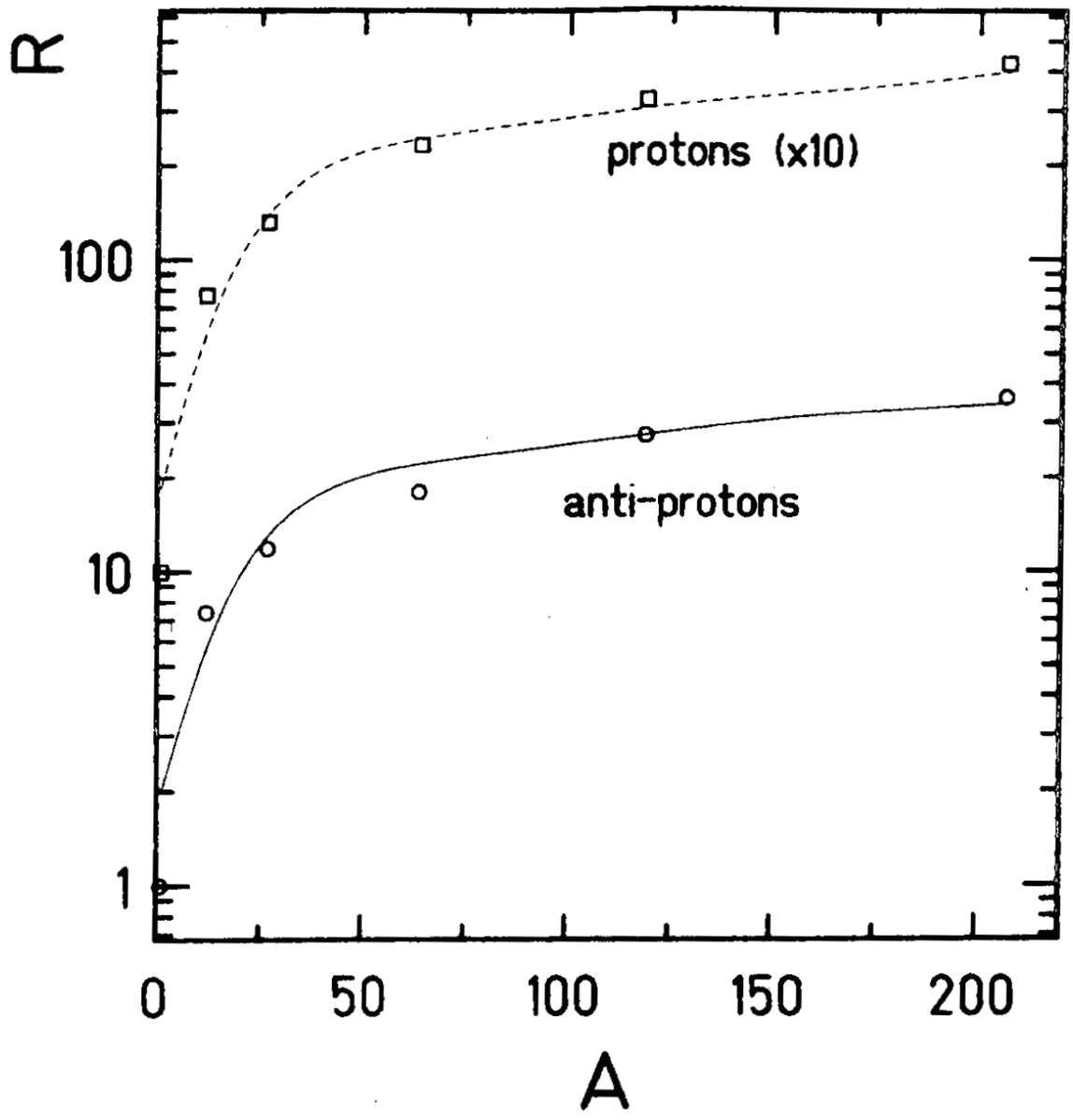

Figure 2

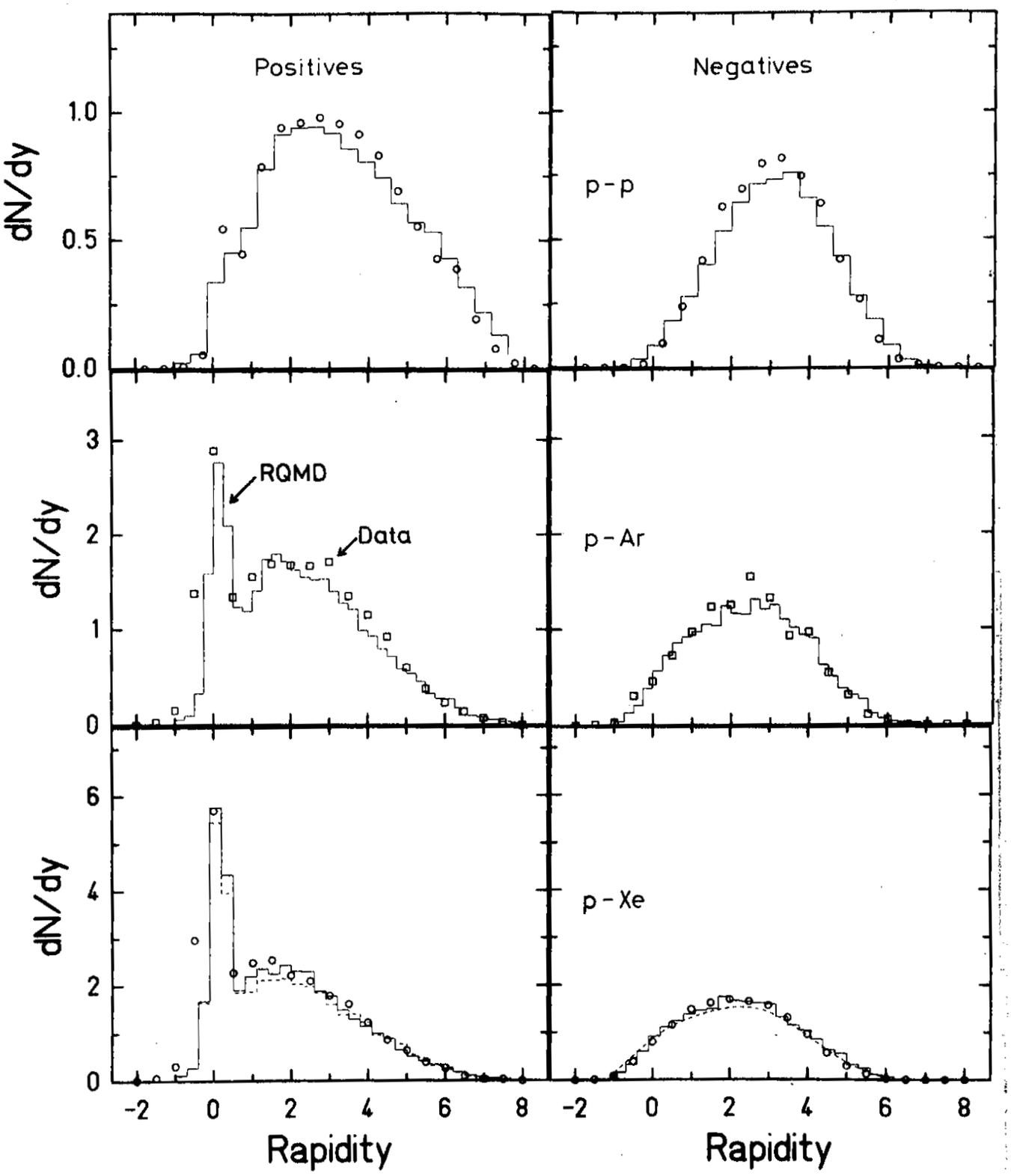
Positives
Negatives
p-p
p-Ar
p-Xe
RQMD
Data
dN/dy
dN/dy
dN/dy
Rapidity
Rapidity
0.0
0.5
1.0
0
1
2
3
0
2
4
6
-2
0
2
4
6
8

Figure 3

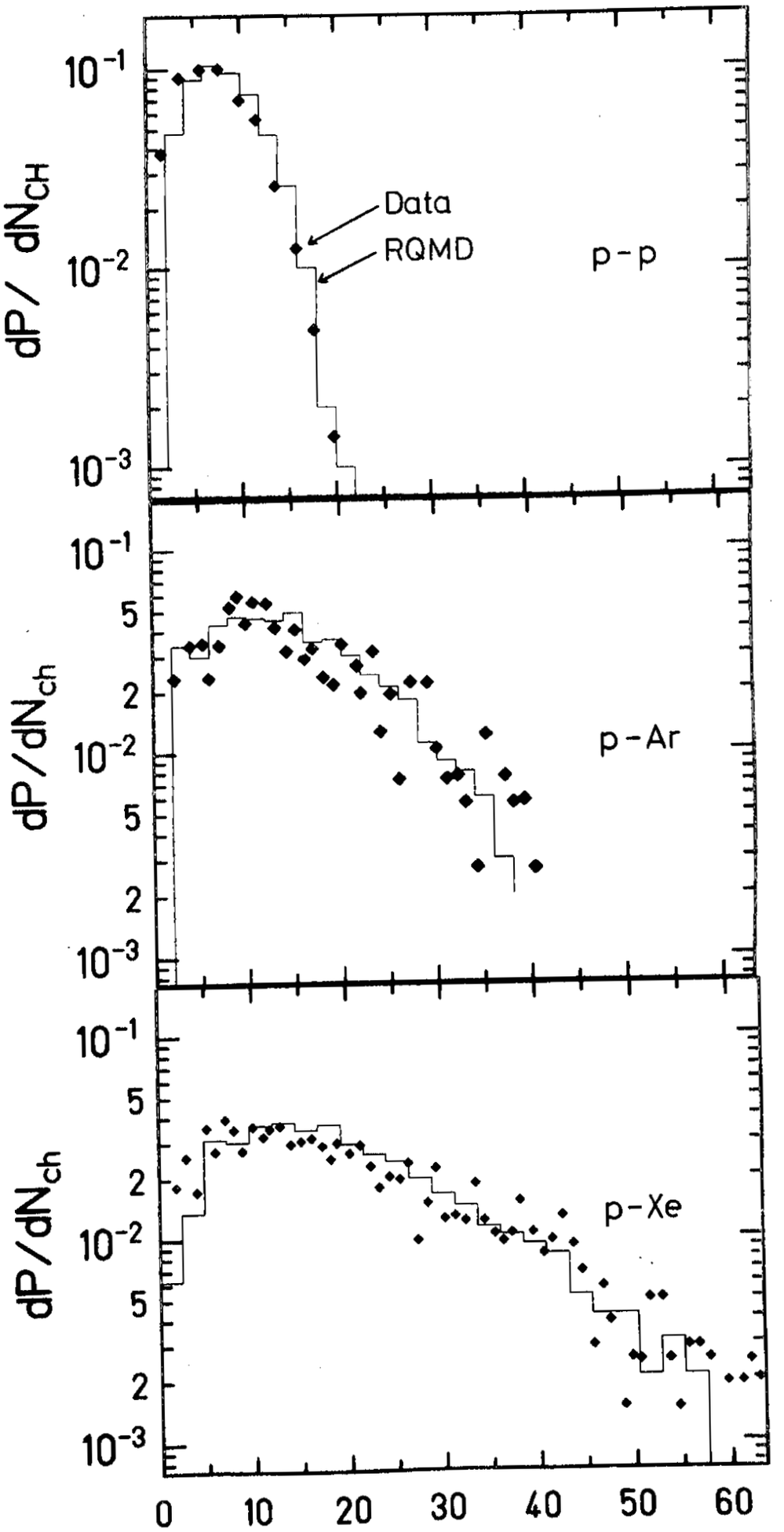
dP/ dN_CH
Data
RQMD
p-p
dP/dN_ch
p-Ar
p-Xe
10^-1
10^-2
10^-3
5
2
0
10
20
30
40
50
60

Figure 4

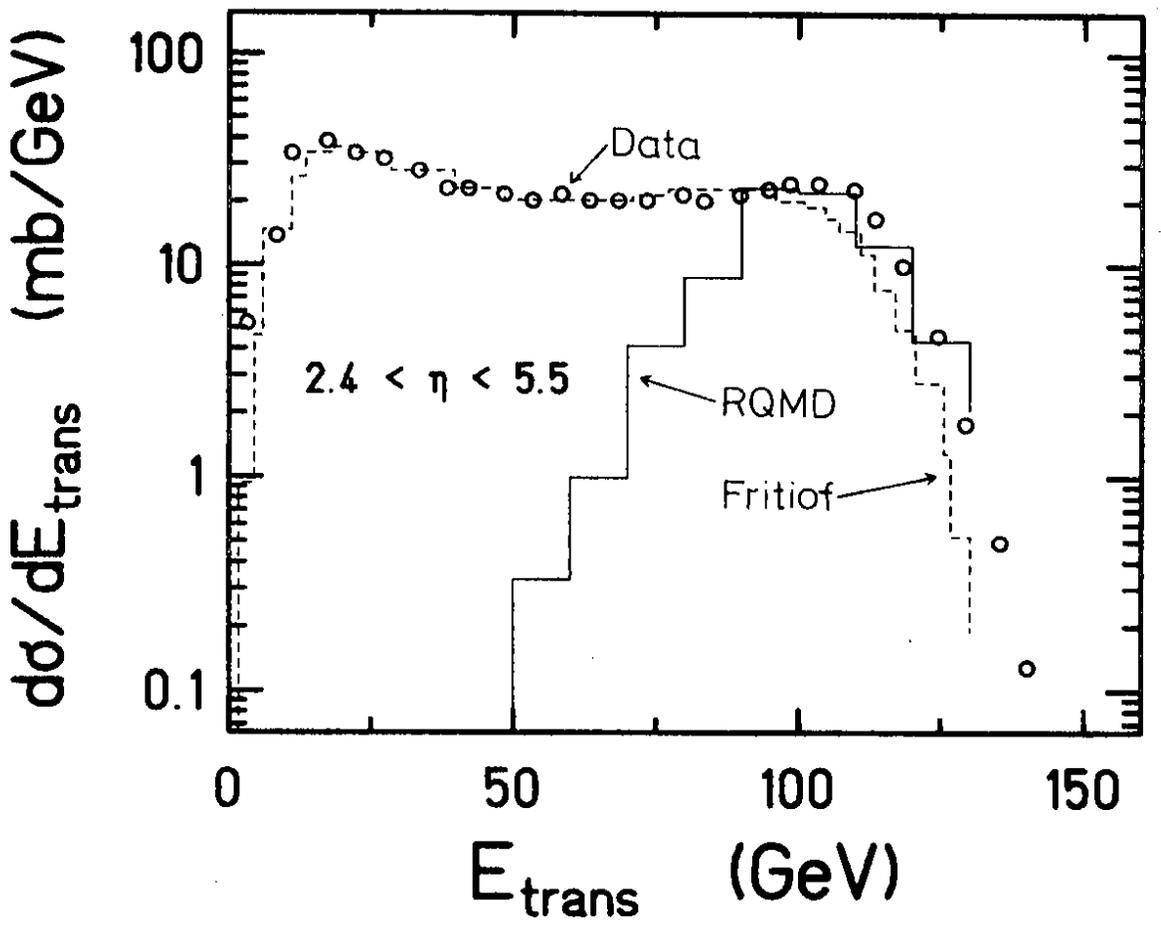
100
10
1
0.1
dσ/dE_trans (mb/GeV)
Data
2.4 < η < 5.5
RQMD
Fritiof
0
50
100
150
E_trans (GeV)

Figure 5

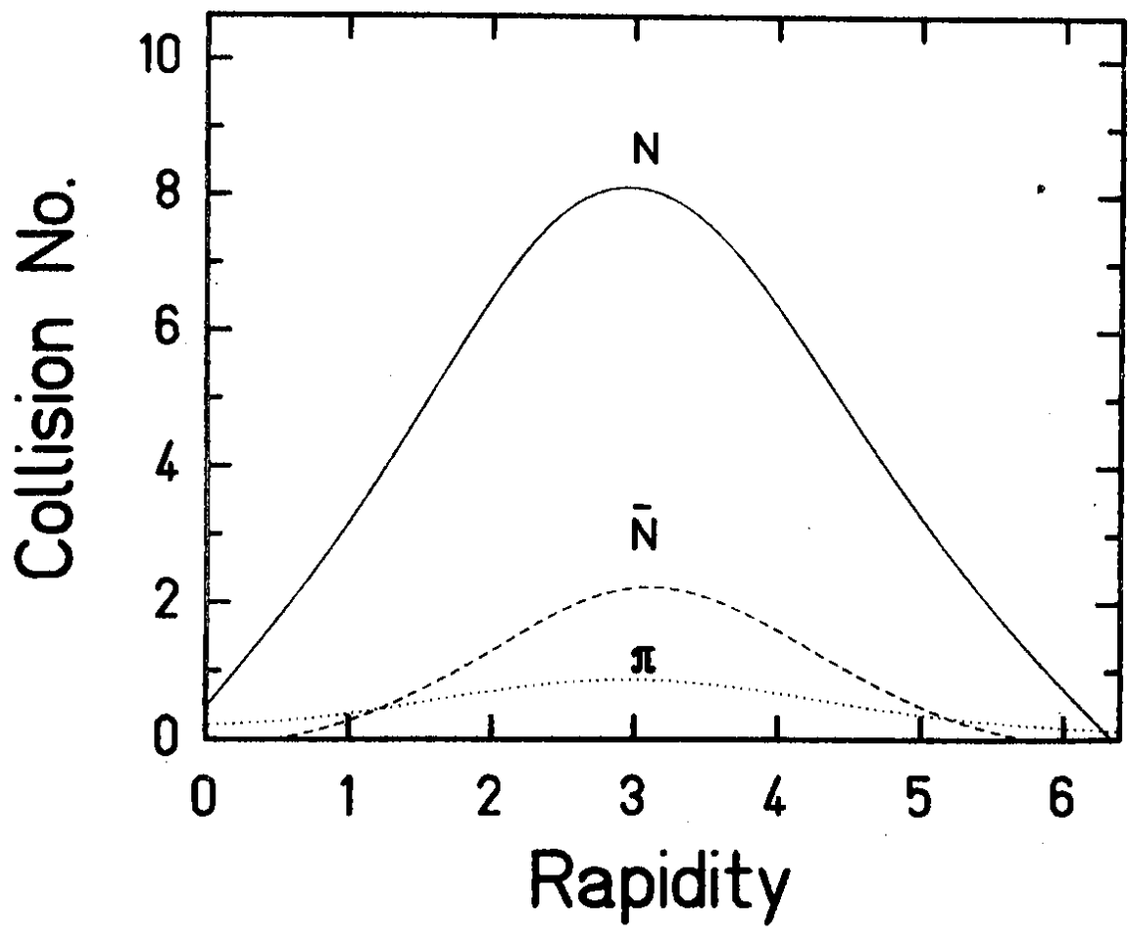

Figure 6

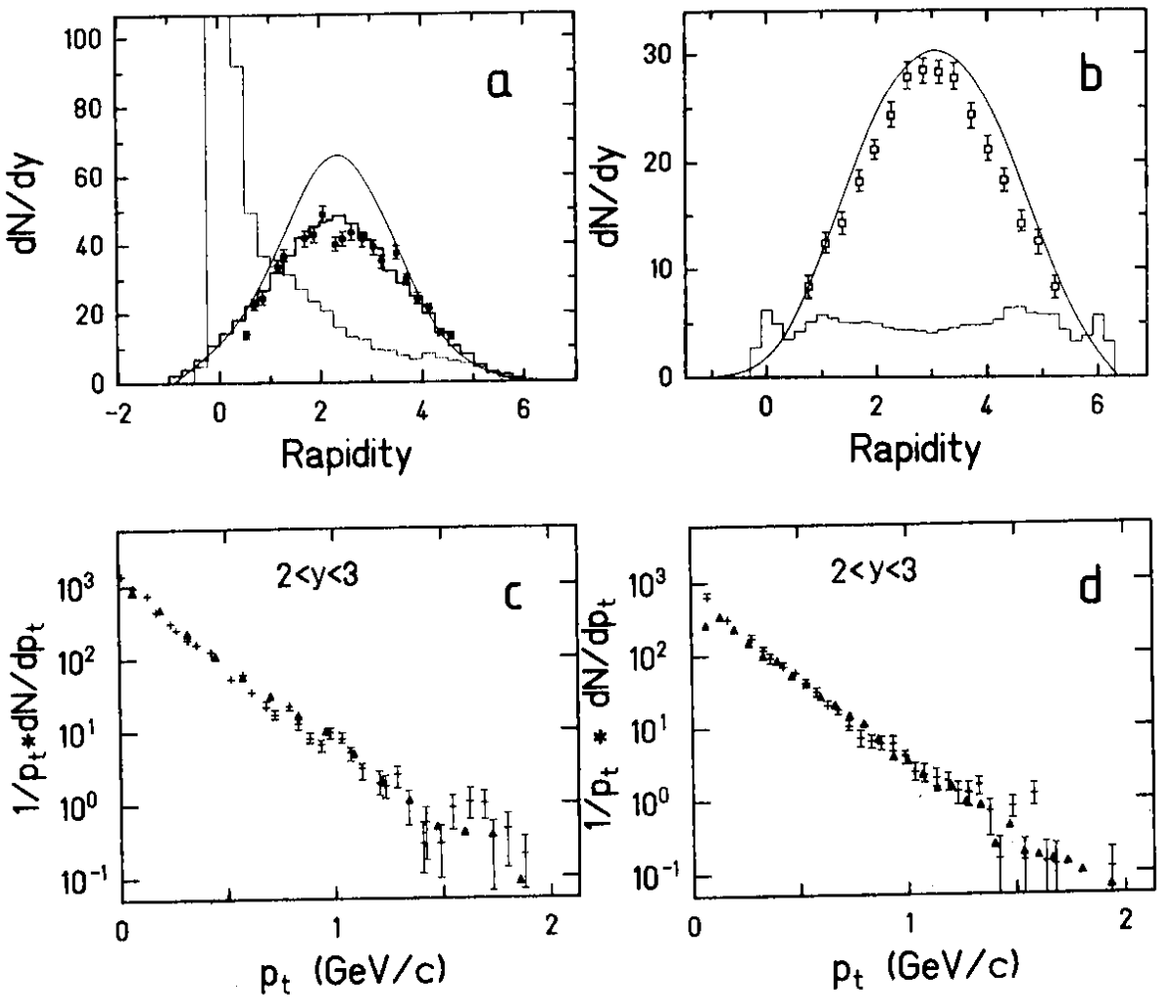

Figure 7